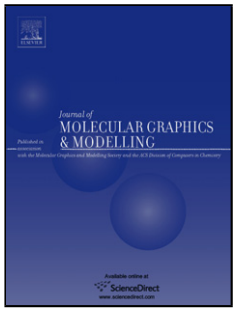

Title: Effect of Graphene Oxide on the Conformational Transitions of Amyloid Beta Peptide: A Molecular Dynamics Simulation Study

Author: Lokesh Baweja Kanagasabai Balamurugan Venkatesan Subramanian Alok Dhawan

PII: S1093-3263(15)30030-9
DOI: http://dx.doi.org/doi:10.1016/j.jmgm.2015.07.007
Reference: JMG 6579

To appear in: *Journal of Molecular Graphics and Modelling*

Received date: 5-3-2015
Revised date: 20-7-2015
Accepted date: 22-7-2015

Please cite this article as: L. Baweja, K. Balamurugan, V. Subramanian, A. Dhawan, Effect of Graphene Oxide on the Conformational Transitions of Amyloid Beta Peptide: A Molecular Dynamics Simulation Study, *Journal of Molecular Graphics and Modelling* (2015), http://dx.doi.org/10.1016/j.jmgm.2015.07.007

- Multiple simulations showed that nanoscale graphene oxide (GO) and reduced graphene oxide (rGO) inhibited the toxic α-helix to β-sheet transitions of amyloid beta (Aβ) peptide.

- The adsorption of Aβ on GO was dominated by electrostatic interactions, whereas both van der Waals and electrostatic interactions contributed in the adsorption of Aβ on rGO.

- rGO was more effective in inhibiting the conformational transitions and dynamics of Aβ due to the increase in hydrophobic π regions as suggested by conformational entropy and secondary structure analysis.

Effect of Graphene Oxide on the Conformational Transitions of Amyloid Beta Peptide: A Molecular Dynamics Simulation Study

Lokesh Baweja[1, 2, 4], Kanagasabai Balamurugan[3], Venkatesan Subramanian[2, 3]

and Alok Dhawan[2, 4#]

[1]Institute of Life Sciences, School of Science and Technology, Ahmedabad University, University Road, Ahmedabad-380009, Gujarat, India.

[2]Academy of Scientific and Innovative Research, Anusandhan Bhavan, 2 Rafi Marg, New Delhi-110001, India.

[3]CSIR-Central Leather Research Institute, Sardar Patel Road, Adyar, Chennai-600020, Tamil Nadu, India.

[4]CSIR-Indian Institute of Toxicology Research, Mahatma Gandhi Road, P.O. Box. 80, Lucknow-226001, Uttar Pradesh, India.

 # To whom correspondence should be addressed:

Professor Alok Dhawan
CSIR-Indian Institute of Toxicology Research
Mahatma Gandhi Road, P.O Box. 80
Lucknow-226001, Uttar Pradesh, India
Email address: alokdhawan@iitr.res.in, alokdhawan@yahoo.com

Abstract:

The interactions between nanomaterials (NMs) and amyloid proteins are central to the nanotechnology-based diagnostics and therapy in neurodegenerative disorders such as Alzheimer's and Parkinson's. Graphene oxide (GO) and its derivatives have shown to modulate the aggregation pattern of disease causing amyloid beta (Aβ) peptide. However, the mechanism is still not well understood. Using molecular dynamics simulations, the effect of graphene oxide (GO) and reduced graphene oxide (rGO) having Carbon:Oxygen ratio of 4:1 and 10:1, respectively, on the conformational transitions (alpha-helix to beta-sheet) and the dynamics of the peptide was investigated. GO and rGO decreased the beta-strand propensity of amino acid residues in Aβ. The peptide displayed different modes of adsorption on Go and rGO. The adsorption on GO was dominated by electrostatic interactions, whereas on rGO, both van der Waals and electrostatic interactions contributed in the adsorption of the peptide. Our study revealed that the slight increase in the hydrophobic patches on rGO made it more effective inhibitor of conformational transitions in the peptide. Alpha helix-beta sheet transition in Aβ peptide could be one of the plausible mechanism by which graphene oxide may inhibit amyloid fibrillation.

Keywords: Graphene oxide, amyloid beta peptide, nanomaterials, molecular dynamics simulation, neurodegenerative disorders

1 Introduction:

Graphene oxide (GO) based nanomaterials (NMs) have been widely recognized as potential candidates in biomedical applications such as biosensing, imaging and drug delivery due to their unique physiochemical properties [1, 2]. GO is a two-dimensional structure consisting of epoxide, hydroxyl on the surface and carboxyl at the edges [3]. These functional groups are responsible for the amphiphilic nature of GO and endow promising properties over unfunctionalised, forms of carbon based NMs such as carbon nanotubes and fullerene in biological applications [4]. However, the uses of NMs in human applications have raised concerns about their potential toxicity [5]. In biological environment, the NMs have high affinity for macromolecules such as proteins [6]. The NMs may perturb the native conformation of proteins and lead to undesirable biological consequences such as inhibition of protein function, protein fibrillation and aggregation [7, 8]. This phenomenon in turn depends upon the surface charge, size, and shape of NMs [9]. However, there are proteins and peptides having high plasticity/inherent tendency to misfold and form aggregates linked to neurodegenerative disorders like Alzheimer's and Parkinson's [10]. The isoforms of amyloid beta (Aβ) peptide (1-40) and (1-42) have been shown to involve in pathogenesis of the disease [11]. The Aβ clearance is reduced and it gets accumulated in the brain in Alzheimer's disease. The Aβ peptides generated by β-secretase in alpha helical conformation get converted into beta sheet conformation to form insoluble fibrils, which ultimately lead to amyloid plaques [12]. Nevertheless, different strategies have been proposed so far to reduce the progression of the disease, which includes conformational stabilisation, inhibiting β-secretase and elimination of amyloid peptide through sink effect [13]. It has been shown that NMs may play a prominent role in reducing the severity of the disease by adsorbing amyloid peptide and inhibiting its conformational transitions and fibrillation [14]. However, studies, on the contrary have also shown that NMs may promote protein fibrillation as reviewed by

Fei *et al.*, [15]. The NMs having inhibitory effect on beta sheet formation may modulate the toxic effect of Aβ on neuronal cells [16]. It is also well known that amyloid oligomers having beta sheet conformation are more toxic than mature amyloid fibrils [17]. Recently, the GO has been proposed as amyloid fibrillation inhibitor [18]. However, the GO-Aβ interactions are still not well understood. Therefore, in this study we have investigated the effects of nano-sized (GO) sheet having surface area of 25 nm^2 and reduced graphene oxide (rGO) on the conformational transitions of Aβ peptide using molecular dynamics (MD) simulations. It has been reported in previous studies that smaller GO sheets are more biocompatible than their larger counterparts [19]. Moreover, the MD simulations have been widely preferred to study NMs-protein interactions and the behavior of Aβ peptide in physiological conditions [20-22]. Till date, the structural information on Aβ peptide could only be obtained through nuclear magnetic resonance (NMR) and MD simulations due to the inherent tendency of the peptide to adopt multiple conformations, which makes it difficult to study Aβ structure and dynamics through experiments [23, 24]. Therefore, the MD simulation is a method of choice for studying NMs-Aβ interactions.

In this study, using MD simulations, the effects of surface chemistries of GO on the conformational transitions and dynamics of Aβ peptide was studied. Moreover, the atomistic scale information provided by this study will be useful in designing biocompatible and therapeutically important GO based platform for diseases involving protein misfolding and aggregation.

2. Material and methods:

2.1. Peptide:

The coordinates of the amyloid beta $(A\beta)_{1-40}$ peptide with a sequence of NH_2-DAEFRHDSGYEVHHQKLVFFAEDVGSNKGAIIGLMVGGVV-COOH was taken from the NMR structures determined in aqueous SDS micelles (PDB entry 1BA4) [23]. The Aβ (1BA4) and Aβ50 (obtained after 50 nanoseconds simulation of Aβ) were used to understand the effect of NMs on the conformational transitions and dynamics of the peptide.

2.2. Models of NMs:

Graphene oxide (GO) and reduced graphene oxide (rGO) having surface area 25 nm^2 was built using Gauss View [25]. The surface was randomly decorated with epoxy and hydroxyl groups. The edges of GO consist of the carboxyl groups which were deprotonated to mimic the behavior of GO at physiological pH 7.4. rGO model has lesser functional groups as compared to GO. Carbon to oxygen (C: O) ratio in GO was ~4:1 and that in rGO was ~10:1. These ratios of GO could be obtained experimentally [3]. The GO consisted of 1005 C and 240 O atoms, whereas 1005 C and 100 O atoms were present in rGO. The O atoms were covalently linked with the carbon rings. Parameters of GO and rGO were taken from a previously published study [26]. The Aβ was placed diagonally at a distance of 10.5 Å from the surface of NMs (Figure 4.1).

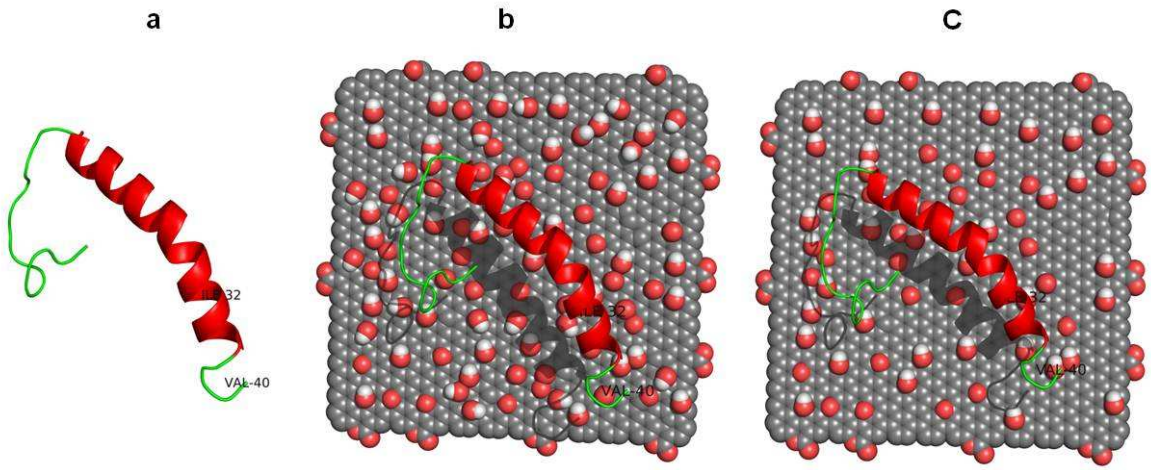

Figure 1: The initial conformations of the system: a) Aβ; b) GO-Aβ; c) rGO-Aβ. The peptide is shown in cartoon representation with red colour. GO and rGO are shown in spherical representation with carbon in grey colour, oxygen and hydrogen in red and white colour, respectively. The red sphere attached with white sphere represents hydroxyl group and red sphere present alone represent the epoxy group.

The side chains of positively charged amino acid residues Lys 28, Arg 5, His 13, 14 and His 6 present in Aβ, were oriented towards the NMs in the starting geometries. Considering, the geometry and the residues in the peptide, this orientation is preferred to understand the effects of NMs on the conformational transitions of Aβ. It has been shown in MD simulation studies that the adsorptions of protein on negatively charged surfaces were dominated by the positively charged residues [27]. The most probable Aβ50 orientation on NMs were deduced using patchdock; the docking was performed between Aβ50 and NMs using shape complementarily algorithm of patchdock. The docked poses are shown in Figure 2 (a-c).

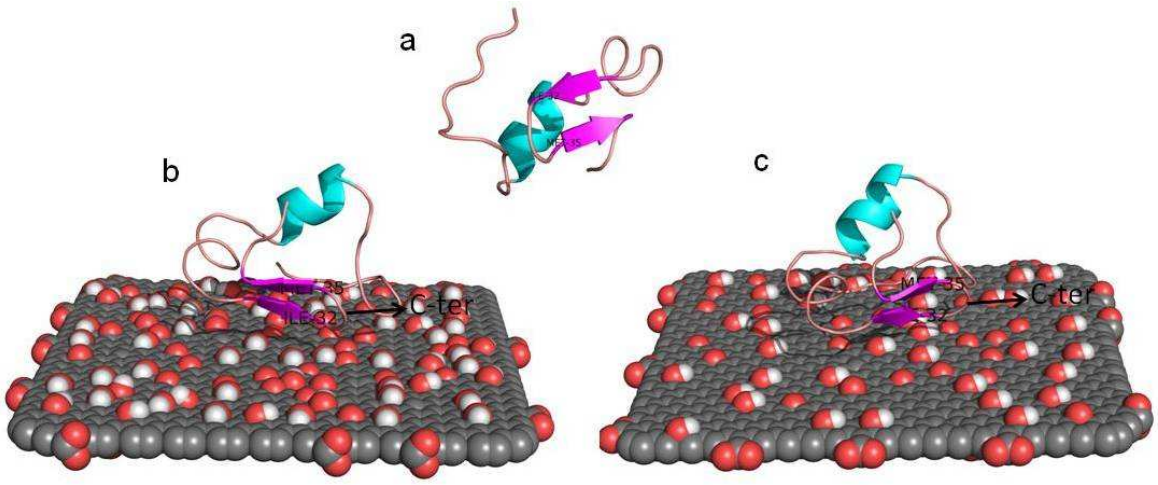

Figure 2: The initial conformation (a) amyloid beta (Aβ50) free in solution, most probable binding site of Aβ50 on NMs; (b) graphene oxide (GO) + Aβ50, (c) reduced graphene oxide (rGO) + Aβ50. The alpha helical region of the peptide is shown in cyan colour, the beta-strands are in magenta colour. The NMs are shown in spherical representation with carbon atoms in grey colour. Oxygen and hydrogen atoms are shown in red and white colour, respectively.

2.3. Molecular dynamics (MD) simulation:

Molecular dynamics simulations were performed using GROMACS-4.5.3 [29]. All simulations were carried out in the isothermal-isobaric ensemble. The pressure was controlled at 1 atm and the temperature was retained at 310 K using Parrinelo-Rahman Barostat and V-rescale thermostat respectively [30-32]. A two femtoseconds (fs) time step was used to integrate the equation of motion. Electrostatic interaction was calculated using Particle Mesh Ewald sums with a non-bonded cut off 10 Å [33]. Bonds between hydrogen and heavy atoms were constrained at their equilibrium length using the linear constraint solver (LINCS) algorithm [34]. Initially, the energy minimizations of the system were carried out followed by the equilibration of all the systems for 200 picoseconds (ps). Later, production runs of 50 ns

were performed in all the systems. The 0.15 M sodium chloride (NaCl) was added to mimic the physiological conditions. The trajectories were saved at 10 ps intervals for further analysis. Analyses of the trajectories were made using GROMACS suite of programs and Visual Molecular Dynamics (VMD) [35]. To understand the NMs induced conformational and structural changes in Aβ peptides, it is important to consider that the chosen force field has an effect on the outcome of the study. It has been shown by Strodel et al that gromos53a6 could reproduce the behavior of Aβ, which was observed in Nuclear Magnet Resonance (NMR) experiments [36]. Therefore, we have chosen gromos53a6 force field for our studies. Moreover, the simulations were performed with randomised velocities. The data from the three simulations was analysed to reach statistical significance.

Table 1: Details of the systems simulated

System Name	**Box Size (nm^3)**	**No. of water molecules/Density(gm/cm^3)(0.15M NaCl)**	**Simulation Time/(Total No. of simulations performed)**
GO (C/O:4/1) + Aβ	11×11×11	56611/1.018	50 ns (3)
rGO(C/O:10/1) + Aβ	11×11×11	56678/1.018	50 ns (3)
Control (Aβ)	10×10×10	43398/1.017	50 ns (3)
GO (C/O:4/1) + Aβ50	11×11×11	56611/1.018	50 ns (3)
rGO (C/O:10/1) + Aβ50	11×11×11	56678/1.018	50 ns (3)
Control (Aβ50)	10×10×10	43398/1.017	50 ns (3)

3. Data Analysis:

The data was analysed from multiple set of trajectories in each system to reach a statistically significant conclusion.

3.1. Radius of gyration:

The radius of gyration analysis was performed using g_gyrate tool in gromacs and used to measure the compactness in the bio-molecules.

3.2. Contact area:

Using g_sas analysis in GROMACS, the contact area between NMs and the peptide was calculated, the area of the molecular surface buried in contact between the two macromolecules is called the interface area or contact area of the molecular assembly.

$$\text{Contact area} = \tfrac{1}{2}\{(SASA_{NM} + SASA_{A\beta} - (SASA_{complex})\}$$

SASA is solvent accessible surface area.

3.3. Quasi harmonic conformational entropy analysis:

The conformational entropy of the Aβ was calculated using g_covar and g_anaeig tools in GROMACS. g_covar was used to superimpose the mainchain atoms of Aβ which calculate and diagonalise the covariance matrix. The –mwa flag was used in g_covar to perform mass weighted covariance analysis, as required by the quasiharmonic entropy calculations. The g_anaeig reads the covariance matrix eigenvectors and calculates the

conformational entropy using the quasi harmonic approximation [38, 39]. The values obtained in J/K-mol are later converted into Kcal/mol.

Quasi harmonic convergence: The estimates of the absolute entropies at the limit of infinite simulation time were calculated using the following equation.

$$S(t) = S_{\infty} - A/t^{n}$$

S_{∞}, A and n are fitting constants and t is the simulation time. We have calculated the entropy of main chain heavy atoms of the peptide from 2 to 50 ns in 2-ns intervals and fit them to the above equation to obtain absolute entropy values to evaluate convergence [38].

3.4 Statistical analysis: The t-test was performed to evaluate the significance between various parameters observed for the peptide.

4. Results and Discussion:

4.1. Secondary structural propensities of Aβ in presence and absence of NMs:

The Aβ structural changes during its interaction with GO and rGO were described using the propensities and percentage of secondary structure elements in Aβ Figure 3(a-c). In the absence of GO and rGO, the N-terminal (1-5) and C-terminal (30-36) residues in the peptide, showed a higher propensity to form β-strand structures. In C-terminal region, the residue's Ile 31 and Ile 32 showed higher propensity (~0.6) to form β-strand conformation. However, in case of GO-Aβ system these values fluctuated between 0.0-0.2, whereas the values in rGO-Aβ system were between 0.0-0.1 with very low standard deviation. This analysis suggested that GO and rGO significantly reduced the β-strand propensity of amino acid residues in Aβ (Figure 4). Further, the percentage of alpha helix and random coil in the peptide showed that the helicity of the peptide was lost in favour of random coil upon interaction with GO and rGO. The percentage of random coil in control, GO-, rGO-Aβ

system increased to 27.5, 55, and 48 %, respectively. The lesser percentage of random coil in control confirmed that the peptide was more structured in absence of NMs (Figure 4).

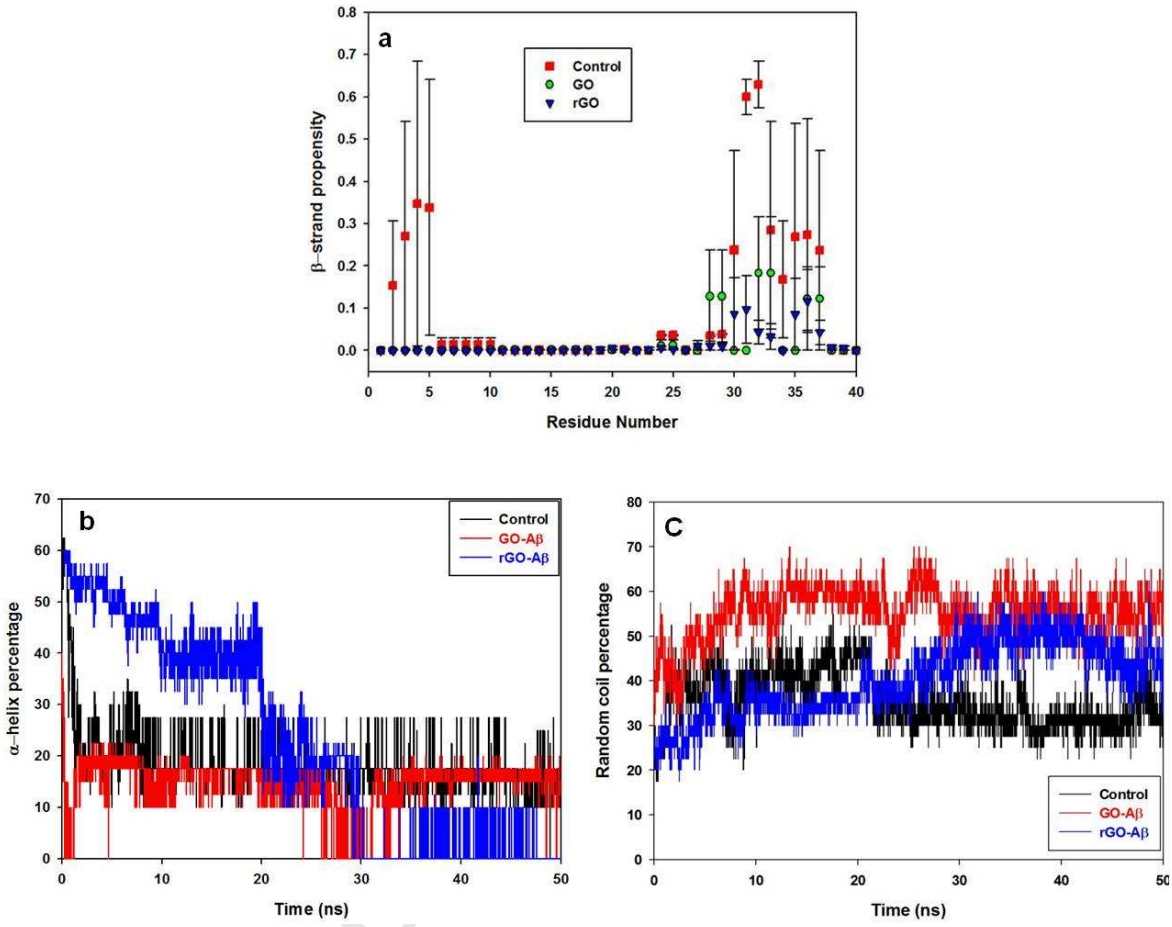

Figure 3: Structural analysis of Aβ in different systems: (a) average values of β-strand propensity of amino acid residues present in Aβ in different systems; (b) time evolution of alpha helical conformation of Aβ; (c) time evolution of random coil conformation of Aβ in different systems.

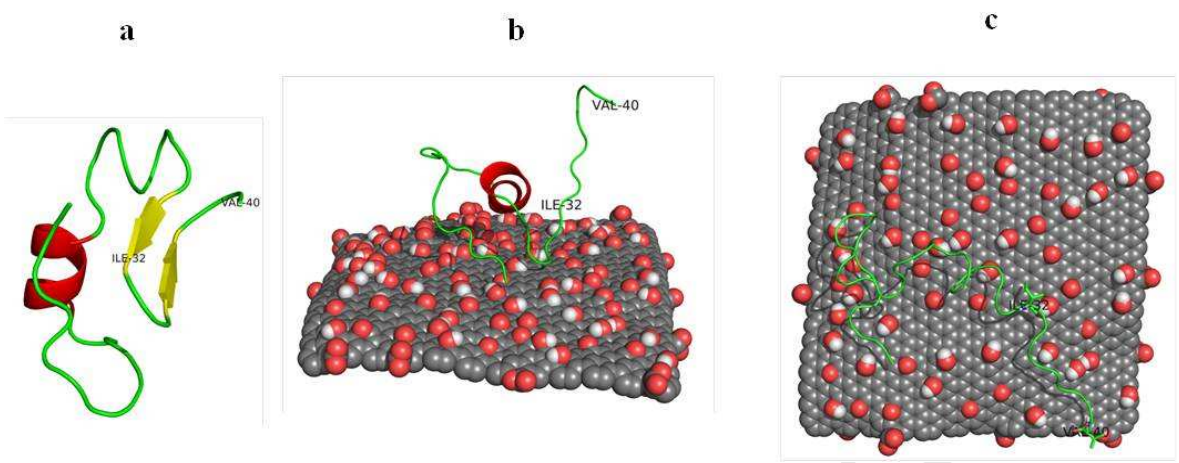

Figure 4: Conformations of amyloid beta (Aβ) obtained at the end of simulations:(a) Control; (b) GO; and (c) rGO.

4.2 Radius of gyration (Rg):

The trend of Rg with respect to time is presented in Figure 5. The average values of Rg over three simulations in GO (4/1)-, rGO (10/1)-Aβ were 1.13±0.07, 1.28±0.03 nm, respectively. t-test analysis showed the significant changes ($p<0.05$) in the Rg values between different systems. Higher values of Rg on rGO suggested the role of surface chemistries in inducing the extended conformations in Aβ. The GO surface is highly negatively charged and has lesser hydrophobic region, whereas rGO has more hydrophobic patches and facilitated the adsorption of C-terminal hydrophobic region which resulted in the extended conformations on rGO (Figure 6). Rg values were in line with the snapshots obtained at the end of the simulation in different systems. The snapshots showed that the rGO induced more extended conformations in Aβ and the C-terminal region interacted favourably with the peptide, whereas the C-terminal region on GO remained exposed to solvent (Figure 6).

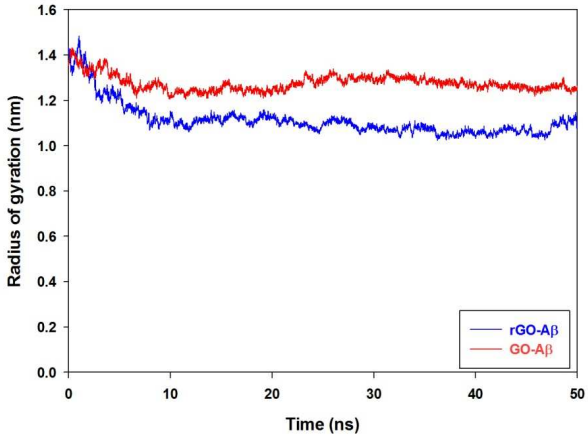

Figure 5: The average values of the radius of gyration (Rg) of Aβ with respect to time in different systems.

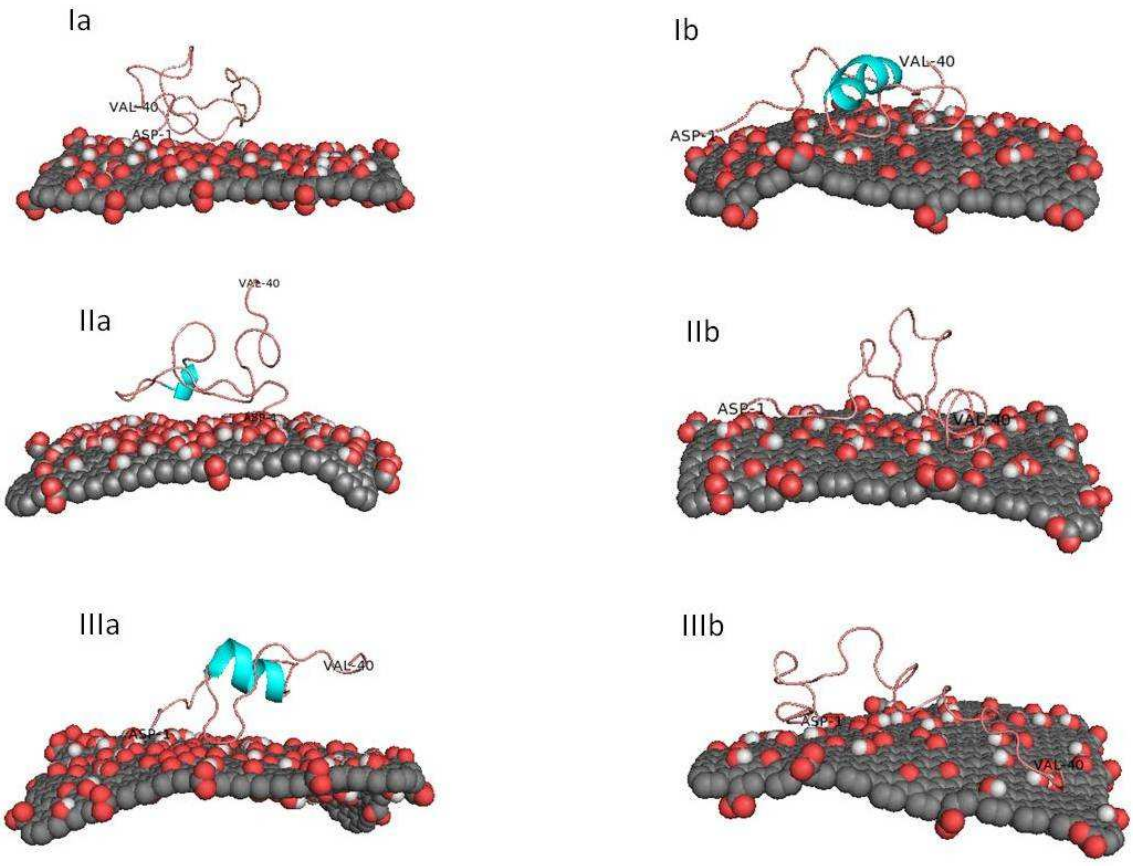

Figure 6: Conformations of amyloid beta (Aβ) obtained at the end of simulations from three different simulations (a) GO and (b) rGO.

4.3. Secondary structural changes in Aβ50 upon interaction with GO (4:1) and rGO (10:1):

The PDB structure 1BA4 obtained from NMR was determined in SDS micelle, which was still far from the conditions used in this study. Further, to clarify whether the inhibition of β-strand conformation in Aβ by NMs is dependent on the initial conformations, the structure of Aβ50 obtained after 50 ns of simulation was taken as a starting geometry. The most probable binding site of Aβ50 on GO and rGO was obtained from patchdock algorithm. This algorithm has been widely used to obtain the initial orientation of proteins (lysozyme) on carbon-based nanomaterials such as carbon nanotubes [40]. The docking results showed that the C-terminal and N-terminal region of the peptide were oriented towards GO and rGO this may be attributed to the shape complementarity between NMs and Aβ50 conformation (Figure 2). Further, the NMs-Aβ50 complexes were simulated for 50 ns and secondary structural propensities obtained from DSSP analysis showed that the percentage of beta-strand conformation increased from 15-25% in control, whereas in GO the β-strand propensity increased from 15-20%. However, the β-strand propensity of the peptide slightly decreased from 15-12.5% (Figure 7). The results were in line with the time evolution of secondary structure plots and the snapshots taken at the end of the simulation (Figure 8 & Figure 9).

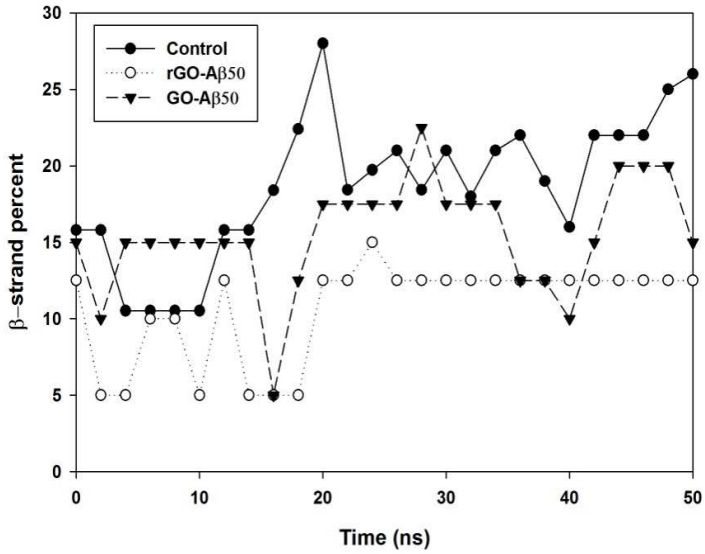

Figure 7: Changes in the β-strand content of Aβ50 with respect to time upon interaction with NMs along with control.

Figure 8: The final conformations of Aβ50 in different systems: (a) Control; (b) GO-Aβ50; (c) rGO-Aβ50.

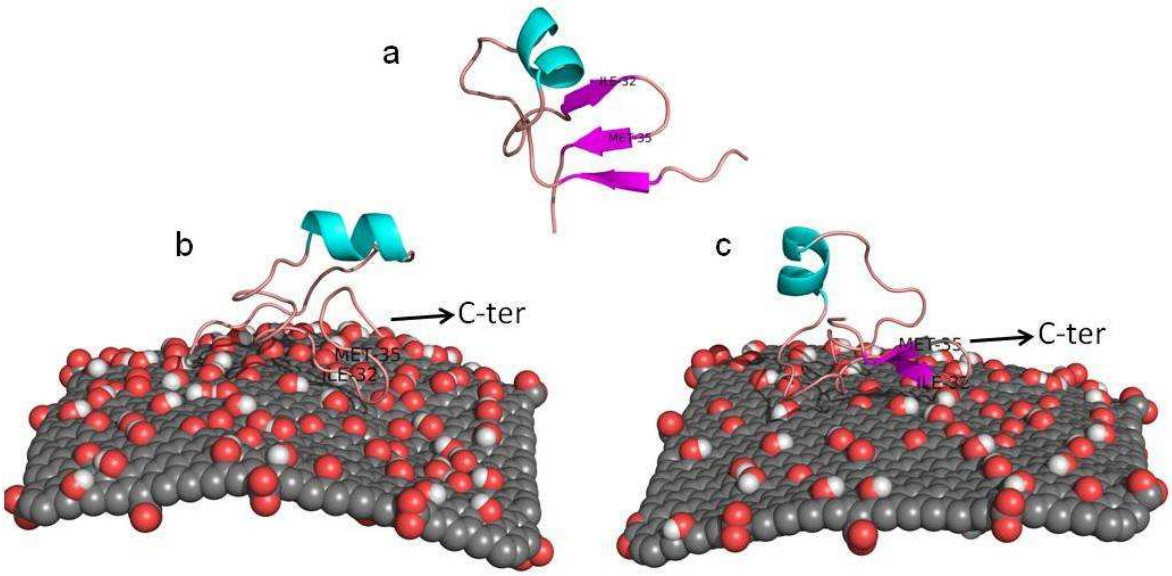

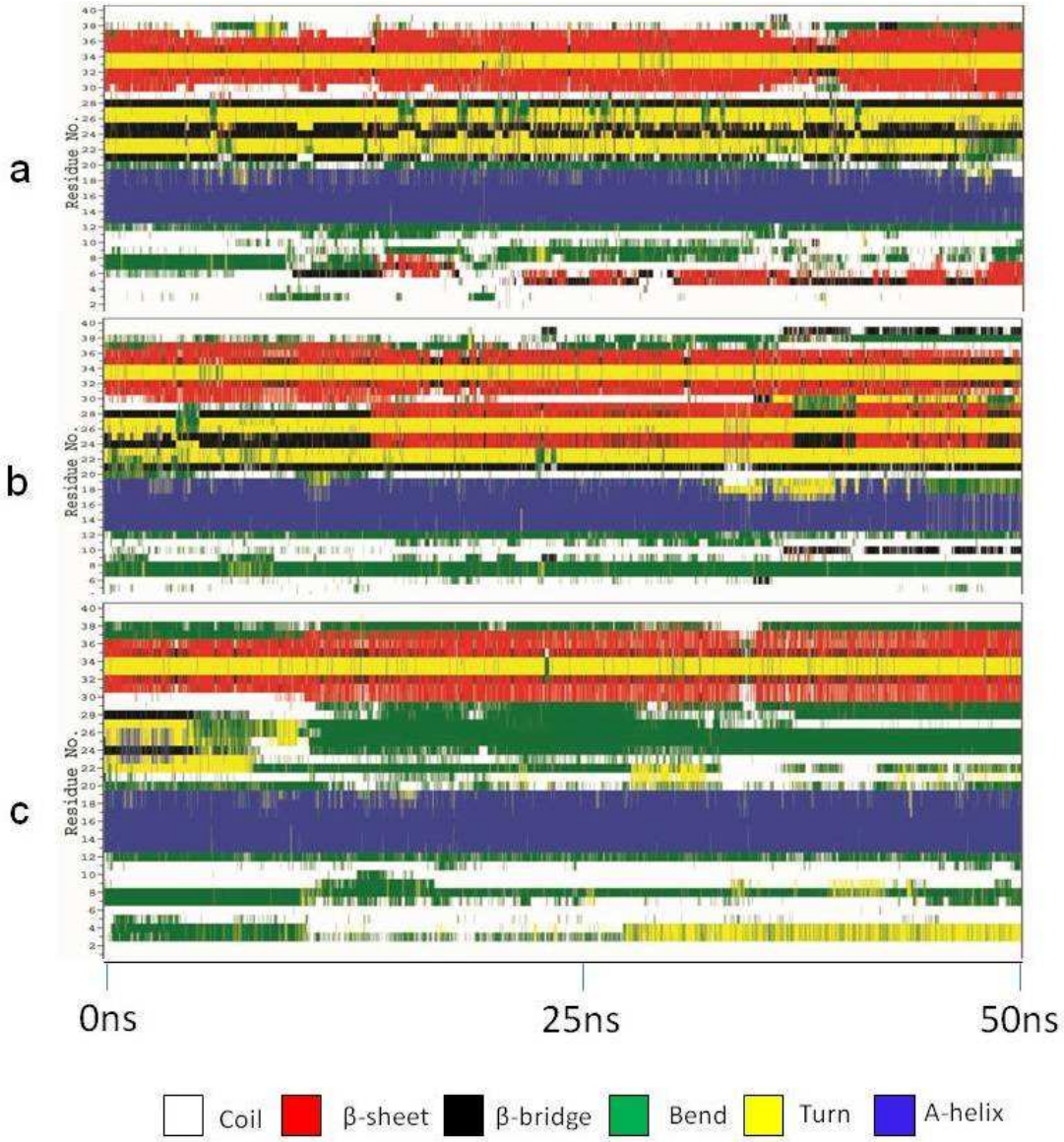

Figure 9: Secondary structure of Aβ50 with respect to time. a) Control; b) GO-Aβ50; c) rGO- Aβ50.

Taking together, the simulations of NMs-Aβ and NMs-Aβ50 complexes showed that the NMs inhibited the conformational transitions of Aβ peptide irrespective of their initial conformation.

4.4. Non-bonded interaction energy analysis:

The adsorption of protein/peptide on NMs is driven by non-covalent interactions such as van der Waals, electrostatic, and hydrophobic [20]. Therefore, the contributions of non-bonded interaction energies between (van der Waals (vdW) and electrostatic) peptide and NMs were analysed and represented in Figure 10 & 11. The adsorption of peptide on GO was driven by electrostatic interactions. In case of rGO-peptide system, the adsorption was driven by both electrostatic and vdW interactions. The mean values of interaction energies are given in Table 2.

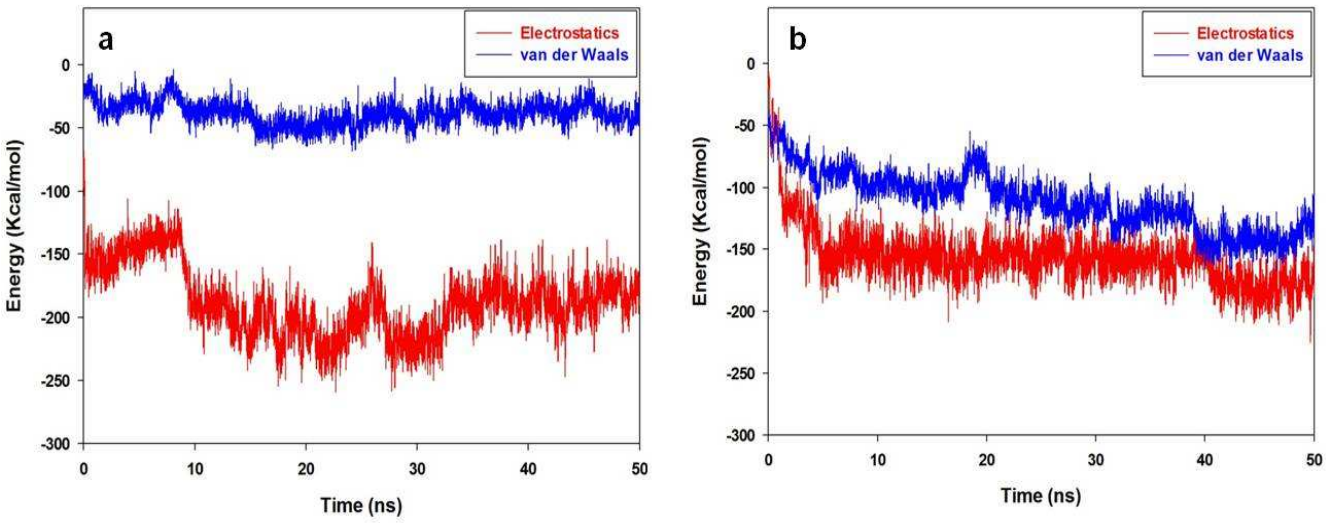

Figure 10: Interaction energy analysis: a) GO-Aβ; b) rGO-Aβ.

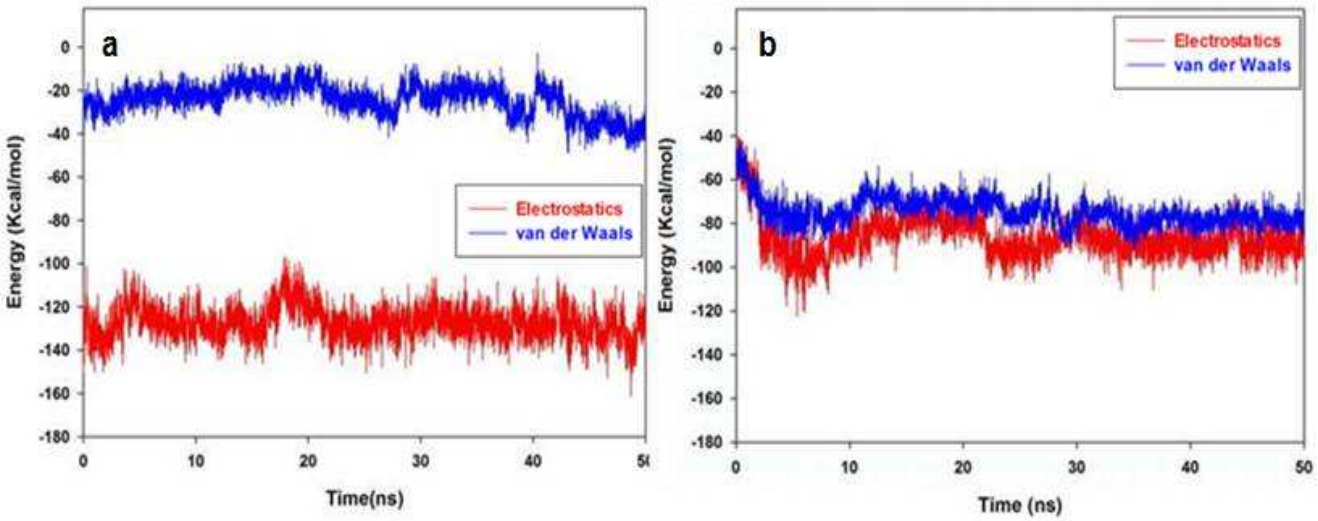

Figure 11: Interaction energy analysis: a) GO-Aβ50; b) rGO-Aβ50.

Table 2: Mean values of energy obtained from different systems.

System (NMs-peptide)	Electrostatic (Kcal/mol)	van der Waals (Kcal/mol)	Total interaction energy (Kcal/mol)
GO-Aβ	-188±27.86	-38.052±9.73	-226±32.24
rGO-Aβ	-155±24.34	-110±23.57	-265±42.30
GO-Aβ50	-127.3±7.67	-24±7.25	-151±10.84
rGO-Aβ50	-74.68±6.43	-86.13±9.70	-161±13.60

The total interaction energy (vdW + Electrostatic) showed the slightly higher affinity of Aβ with rGO. The hydrogen bonds formed between functional groups and positively charged residues in the peptide were contributed in the electrostatic energy (data not shown). The increase in the van der Waals interaction on rGO attributed to the increase in unfunctionalised regions on the surface.

4.5. Conformational entropy analysis:

We have employed quasi harmonic approach to understand the trend of conformational entropy of the peptide in different systems. The principal difficulty when calculating conformational entropy is their convergence. The covariance matrices used in the quasi harmonic approach are difficult to converge in short time intervals used in our study. Therefore, we first evaluated the conformational entropy convergence. The systems showed a lack of convergence (Figure 12).

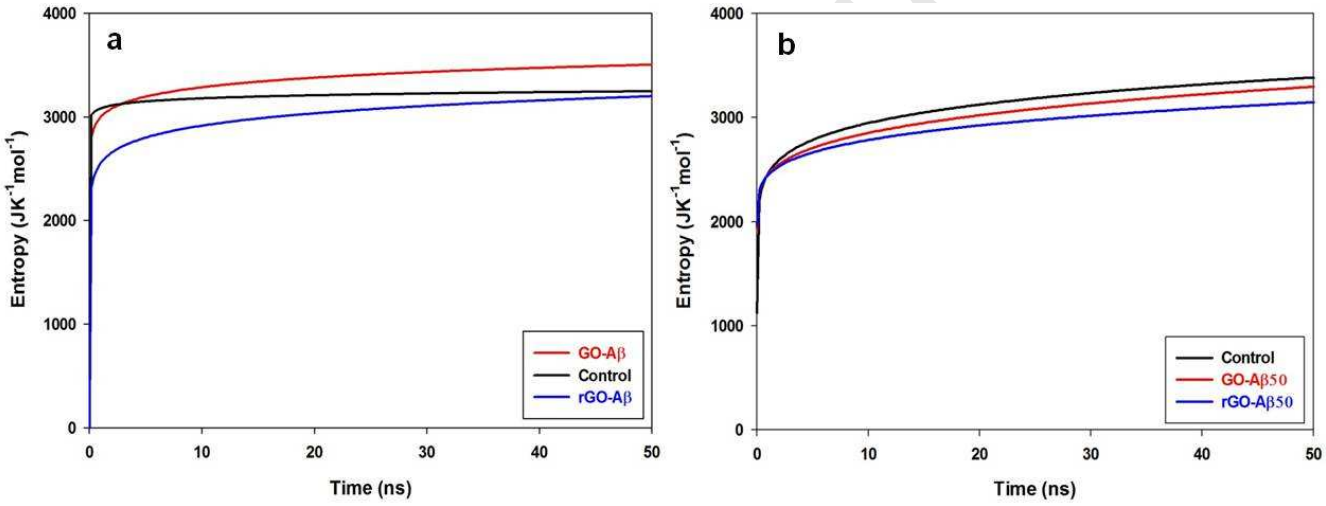

Figure 12: Trend of conformational entropy with respect to time: a) Aβ; b) Aβ50.

Despite lack of convergence, the peptide on rGO exhibited lower conformational entropy values compared to GO. This may be attributed to the differential dynamics of Aβ on NMs as suggested by root mean square fluctuations (RMSF) of Cα atoms. The Aβ on GO showed higher fluctuations (high RMSF values) in C-terminal region that remain exposed towards solvent, whereas this region interacted favourably with rGO and showed low RMSF values (Figure 13 & 6).

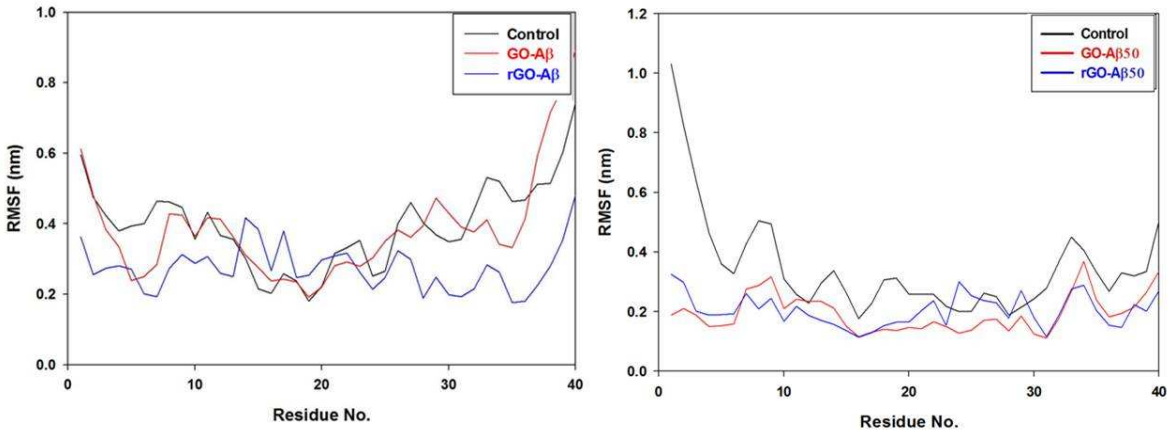

Figure 13: Root mean square fluctuation of Cα atoms: a) Aβ; b) Aβ50.

It has been recently shown that the cross-dimerisation of IDPs reduces the RMSF of the peptide [41]. The calculations in quasi harmonic approximations are based on the motions of the macromolecules and not take into account the self-entropy due to rotation, translational and conformational changes of the molecule [42]. However, the conformational entropy calculated in different systems showed that the surface chemistry of NMs determines the dynamics of IDPs such as Aβ. Therefore, the observed changes in entropy during simulations were not an artifact. Further, we have calculated the entropy loss upon interaction with NMs relative to free Aβ50 per heavy atom of the peptide. The average values were taken to analyse the entropic loss. The marginally higher loss in conformational entropy on rGO could be one of the reasons for its effectiveness towards restricting the dynamics of Aβ.

Table 3: Conformational entropy analysis

System	Entropy(S)(per heavy atom) J/K-mol	S_{free} - $S_{complex}$
Free Aβ50	16.73	_
GO-Aβ50	16.35	0.38
rGO-Aβ50	15.83	0.90

.

5. Discussion:

MD simulations are widely preferred to study biomolecular systems such as amyloid beta peptide monomer and oligomer [20-22]. The convergence/equilibration is one of the major problems in MD simulations. The RMSD is an indicator of system equilibration with time [43]. Therefore, we have calculated the RMSD of the peptide with respect to time. The Cα atoms in the Aβ peptide during initial phase (0-10 ns) of the simulation attained the value of ~1.2, ~1.1 and 0.6 nm, respectively in control, GO, and rGO systems. These values fluctuated with a range of 0.2 nm in the rest of the time. The same trend of RMSD was also observed for Aβ50 (Figure 14)

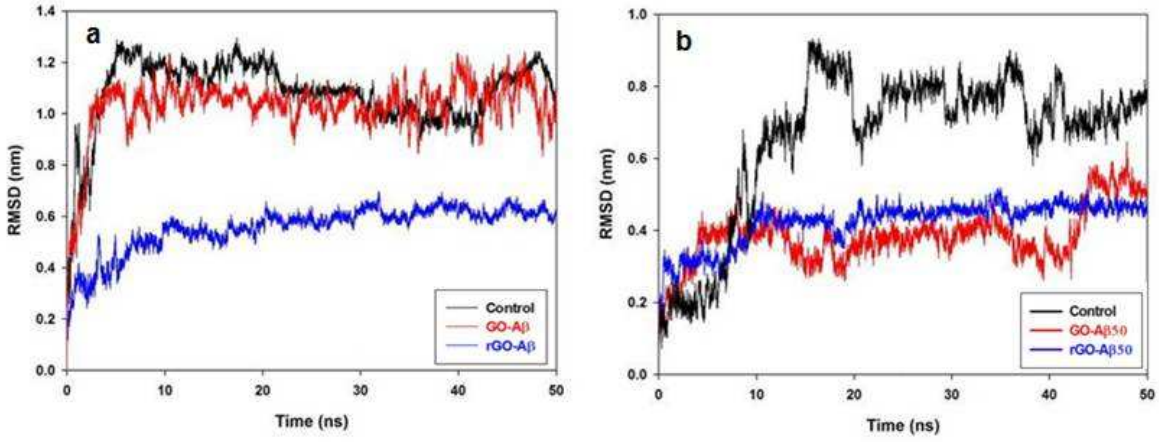

Figure 14: The roots mean square deviation of Cα atoms: (a) Aβ and (b) Aβ50.

The RMSD analyses showed that systems reached equilibration with time. The difference in the RMSD values observed in the different system may be attributed to the different starting conformations of Aβ. Moreover, it has been shown that it is difficult to reach convergence even in 500 ns simulation in case of proteins [44]. Considering this issue, we have performed multiple simulations and used statistical analysis to probe the structural changes and dynamics of the peptide in different systems. Nanomaterials (NMs) have been shown to modulate the aggregation of Aβ peptide [15]. Most of the experimental studies showed that NMs binds with the amyloid monomer and inhibits the aggregation through monomer competition mechanism [8]. The similar mechanism has also been proposed for GO [18]. However, the effects of NMs on the conformational transitions and dynamics of Aβ are still not well understood. α-helix to β-sheet transitions are considered as the initial step in amyloid aggregation [13]. We probed using MD simulation that the adsorption of Aβ on GO and rGO inhibited its tendency to acquire β-sheet conformation. However, Aβ exhibited different adsorption mechanisms on NMs that may be attributed to the surface chemistries of NMs. The electrostatic interactions were more pronounced on GO, whereas both van der Waals and electrostatic interactions play a major role in the adsorption of Aβ on rGO. It has been shown that amyloid inhibitors proteins such as lysozyme inhibited the fibrillation of Aβ, which interacted with the peptide through electrostatic, and van der Waals interaction and lead to the conformational stabilization of Aβ [45]. This could be the one of the reasons for the efficient inhibition Aβ conformational transition by rGO, due to the formation of favourable van der Waals and electrostatic interactions with Aβ. Moreover, it has been shown in previous studies that hydrophobic NMs such as carbon nanotubes and fullerene can efficiently bind and inhibit the β-sheet tendency of IDPs [46]. This study suggested the role of hydrophobicity in inhibiting the β-sheet formation. The hydrophobic interactions between NMs-protein interfaces can be understood in terms of contact area.

The higher contact area between rGO-Aβ interfaces could be attributed to the increase in the hydrophobic π regions on the surface rGO (Figure 15). It can be clearly observed from that GO-Aβ50 interface is highly hydrated as compared to rGO-Aβ50, which means that the adsorption of Aβ50 on hydrophobic π regions displaced more water molecules as shown in Figure 16.

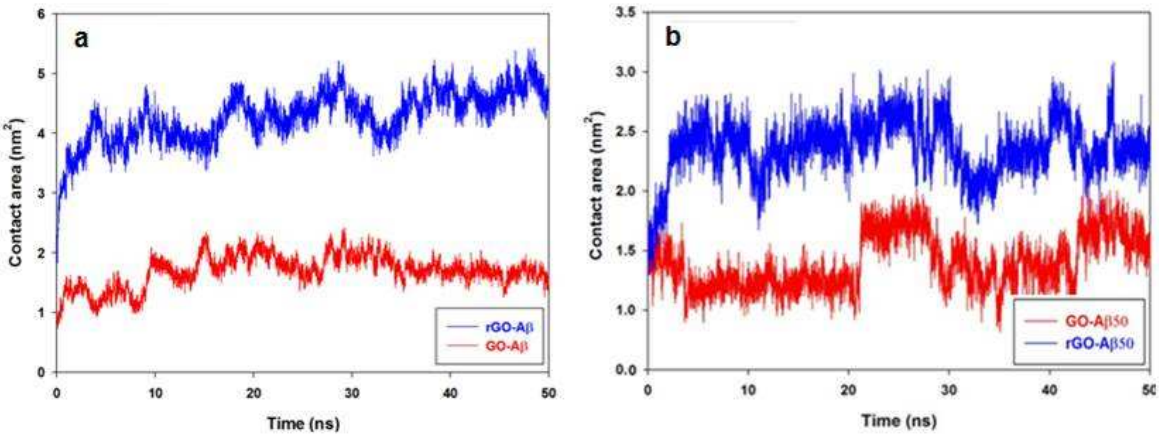

Figure 15: Contact area with respect to time: a) Aβ; b) Aβ50.

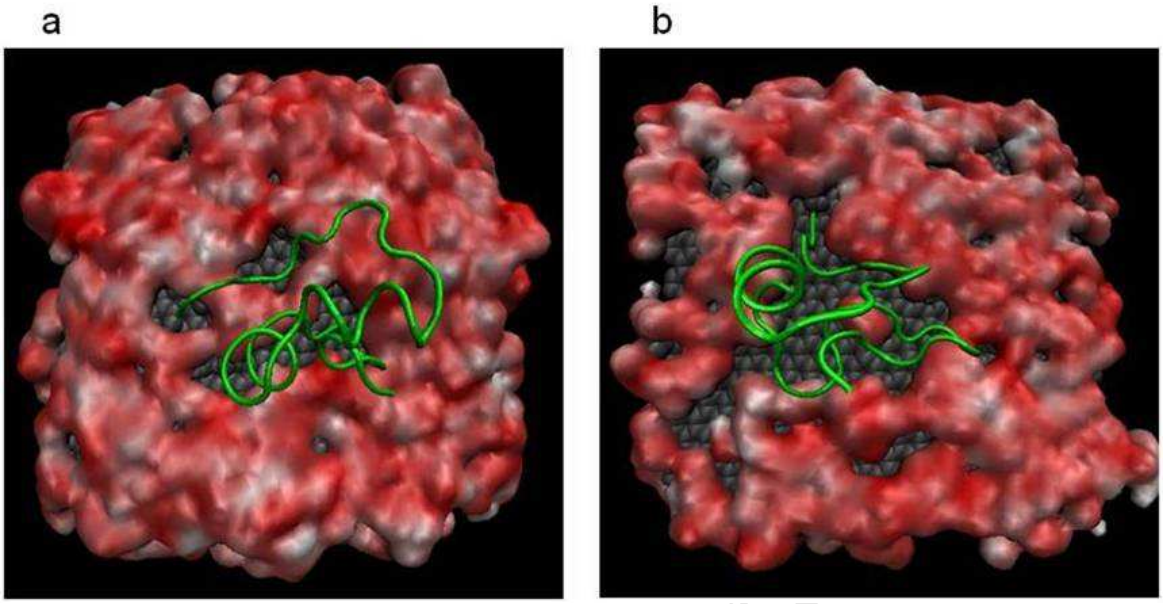

Figure 16: Hydration patterns of final NMs-Aβ50 complexes: (a) GO-Aβ50 (b) rGO-Aβ50. The GO-Aβ50 interface is highly hydrated as compared to rGO-Aβ50 interface. The NMs are shown in grey colour, water in surface representation and protein in green colour.

The increase in hydrophobic interactions between rGO and Aβ could be one of the reasons for the effective conformational stabilization. The existence of the water molecules between hydrophobic moieties is entropically unfavourable and could be responsible for the higher dehydration of rGO-Aβ50 interface and in line with our previous findings [20]. The analyses such as conformational entropy, contact area, and secondary structural showed that the rGO was more effective in inhibiting the conformational transitions in Aβ. Moreover, the C: O ratios used in this study were higher than the experimental ratio of GO ~1.67/1 and ~2/1. There are the following reasons: It has been shown that highly electronegative surfaces may nucleate the pathogenic assembly of Aβ [47]. Moreover, it has been shown that NMs having both hydrophilic and hydrophobic interactions with Aβ are more efficient in inhibiting the

toxicity of Aβ [48, 49]. This possibility can be achieved with GO having slightly higher C: O ratios as suggested by this simulation study.

6. Conclusion:

The salient features emerged from this study are as follows:

1. Graphene based nanomaterials GO and rGO could inhibit the toxic α-helix to β-sheet transitions of amyloid beta peptide.
2. The rGO was more efficient in inhibiting the α-helix to β-sheet this could be attributed to the increase in hydrophobic π regions on rGO surface.
3. The inhibition of conformational transitions is independent of the initial conformation of Aβ.
4. Overall, the study suggested that nanoscale graphene oxide may modulate the early stages of amyloid fibrillation.

7. Acknowledgements:

LB would like to thank the University Grant Commission (UGC), New Delhi for providing Senior Research Fellowship. The funding from Department of Biotechnology, Government of India under the NewINDIGO Scheme for NanoLINEN project is gratefully acknowledged. The funding received from the Council of Scientific and Industrial Research, New Delhi (NWP-35); the UK India Education and Research Initiative (UKIERI) standard award to the Institute of Life Sciences, Ahmedabad University, India (grant No. IND/CONT/E/11-12/217) and from EU Framework Programme (FP7/2007-2013) under grant agreement No. 263147 (NanoValid - Development of reference methods for hazard identification, risk assessment and LCA of engineered nanomaterials) is also acknowledged. The financial assistance for the Centre for Nanotechnology Research and Applications (CENTRA) by The Gujarat Institute for Chemical Technology (GICT) is also acknowledged.

8. References:

1. Wang, Y.; Li, Z.; Wang, J.; Li, J.; Lin, Y., Graphene and Graphene oxide: Biofunctionalization and Applications in Biotechnology. *Trends Biotechnol* **2011**, *29*, 205-212.

2. Liu, J.; Cui, L.; Losic, D., Graphene and Graphene Oxide as New Nanocarriers for Drug Delivery Applications. *Acta Biomater* **2013**, *9*, 9243-9257.

3. Dreyer, D. R.; Park, S.; Bielawski, C. W.; Ruoff, R. S. The Chemistry of Graphene Oxide. *Chem. Soc. Rev* **2010**, *39*, 228-240.

4. Bussy, C.; Ali-Boucetta, H.; Kostarelos, K., Safety Considerations for Graphene: Lessons Learnt from Carbon Nanotubes. *Acc Chem Res* **2012**, *46*, 692-701.

5. Sharifi, S.; Behzadi, S.; Laurent, S.; Forrest, M. L.; Stroeve, P.; Mahmoudi, M., Toxicity of Nanomaterials. *Chem Soc Rev* **2012**, *41*, 2323-2343.

6. Shemetov, A. A.; Nabiev, I.; Sukhanova, A. Molecular Interaction of Proteins and Peptides with Nanoparticles. *ACS Nano* **2012**, *6*, 4585-4602.

7. Zhang, D. M.; Neumann, O.; Wang, H.; Yuwono, V. M.; Barhoumi, A.; Perham, M.; Hartgerink, J. D.; Wittung-Stafshede, P.; Halas, N. J. Gold Nanoparticles can Induce the Formation of Protein-Based Aggregates at Physiological pH. *Nano Lett* **2009**, *9*, 666-671.

8. Li, C.; Mezzenga, R., The Interplay between Carbon Nanomaterials and Amyloid Fibrils in Bio-nanotechnology. *Nanoscale* **2013**, *5*, 6207-6218.

9.Skrabana, R.; Sevcik, J.; Novak, M., Intrinsically Disordered Proteins in the Neurodegenerative Processes: Formation of Tau Protein Paired Helical Filaments and their Analysis. *Cell Mol Neurobiol* **2006**, *26*, 1085-1097.

10. Albanese, A.; Tang, P. S.; Chan, W. C., The Effect of Nanoparticle Size, Shape, and Surface Chemistry on Biological Systems. *Annu Rev Biomed Eng* **2012**, *14*, 1-16.

11. Sisodia, S. S.; Price, D. L., Role of the Beta-amyloid Protein in Alzheimer's Disease. *Faseb J* **1995**, *9*, 366-370.

12. Kayed, R.; Head, E.; Thompson, J. L.; McIntire, T. M.; Milton, S. C.; Cotman, C. W.; Glabe, C. G., Common Structure of Soluble Amyloid Oligomers implies Common Mechanism of Pathogenesis. *Science* **2003**, *300*, 486-489.

13. Gandy, S.; DeKosky, S. T., Toward the Treatment and Prevention of Alzheimer's Disease: Rational Strategies and Recent Progress. *Annu Rev Med* **2013**, *64*, 367-383.

14. Brambilla, D. et al, PEGylated Nanoparticles Bind to and Alter Amyloid-beta Peptide Conformation: Toward Engineering of Functional Nanomedicines for Alzheimer's Disease. *ACS Nano* **2012**, *6*, 5897-908.

15. Fei, L.; Perrett, S., Effect of Nanoparticles on Protein Folding and Fibrillogenesis. *Int J Mol Sci* **2009**, *10*, 646-655.

16. Liao, Y. H.; Chang, Y. J.; Yoshiike, Y.; Chang, Y. C.; Chen, Y. R., Negatively Charged Gold Nanoparticles inhibit Alzheimer's Amyloid-beta Fibrillization, induce Fibril Dissociation, and Mitigate Neurotoxicity. *Small*, **2013**, *8*, 3631-3639.

17. Ladiwala, A. R.; Litt, J.; Kane, R. S.; Aucoin, D. S.; Smith, S. O.; Ranjan, S.; Davis, J.; Van Nostrand, W. E.; Tessier, P. M., Conformational Differences between two Amyloid Beta Oligomers of Similar Size and Dissimilar Toxicity. *J Biol Chem*, **2012**, *287*, 24765-24773.

18. Mahmoudi, M.; Akhavan, O.; Ghavami, M.; Rezaee, F.; Ghiasi, S. M., Graphene oxide Strongly Inhibits Amyloid Beta Fibrillation. *Nanoscale*, **2013**, *4*, 7322-7325.

19. Pei, X.; Wang, J.; Wan, Q., Comment on "Amine-Modified Graphene: Thrombo-protective Safer Alternative to Graphene Oxide for Biomedical Applications". *ACS Nano*, **2014**, *8*, 1966.

20. Baweja, L.; Balamurugan, K.; Subramanian, V.; Dhawan, A., Hydration Patterns of Graphene-Based Nanomaterials (GBNMs) Play a Major Role in the Stability of a Helical protein: A Molecular Dynamics Simulation Study. *Langmuir* **2013**, *29*, 14230-14238

21. Makarucha, A. J.; Todorova, N.; Yarovsky, I. Nanomaterials in Biological Environment: A Review of Computer Modelling Studies. *Eur. Biophys. J.* **2011**, *40*, 103-115.

22. Lemkul, J. A.; Bevan, D. R., The Role of Molecular Simulations in the Development of Inhibitors of Amyloid Beta-Peptide Aggregation for the Treatment of Alzheimer's Disease. *ACS Chem Neurosci* **2012**, *3*, 845-856

23. Coles, M.; Bicknell, W.; Watson, A. A.; Fairlie, D. P.; Craik, D. J., Solution Structure of Amyloid Beta-Peptide(1-40) in a Water-Micelle Environment. Is the Membrane-Spanning Domain Where We Think It Is? *Biochemistry* **1998**, *37*, 11064-11077.

24. Xu, Y.; Shen, J.; Luo, X.; Zhu, W.; Chen, K.; Ma, J.; Jiang, H., Conformational Transition of Amyloid Beta-Peptide. *Proc Natl Acad Sci U S A* **2005**, *102*, 5403-5407.

25. GaussView; Gaussian, Inc.: Pittsburgh, PA, **2003**

26. Shih, C. J.; Lin, S. C.; Sharma, R.; Strano, M. S.; Blankschtein, D. Understanding the pH-Dependent Behavior of Graphene Oxide Aqueous Solutions: A Comparative Experimental and Molecular Dynamics Simulation Study. *Langmuir* **2012**, *28*, 235-241.

27. Liu, J.; Liao, C.; Zhou, J., Multiscale Simulations of Protein G B1 Adsorbed on Charged Self-Assembled Monolayers. *Langmuir* **2013**, *29*, 11366-11374.

28.Schneidman-Duhovny, D.; Inbar, Y.; Nussinov, R.; Wolfson, H. J., PatchDock and SymmDock: Servers for Rigid and Symmetric Docking. *Nucleic acids research* **2005**, *33*, 363-367.

29. Lindahl, E.; Hess, B.; van der Spoel, D., GROMACS 3.0: A Package for Molecular Simulation and Trajectory Analysis. *J. Mol. Model.* **2001**, *7*, 306-317

30. Parrinello, M., Rahman, A., Polymorphic Transitions in Single Crystals: A New Molecular

Dynamics Method. *J. App. Phys.* **1981**, *52*, 7182-7190.

31. Nosé, S., Klein,M.L., A Unified Formulation of the Constant Temperature Molecular Dynamics Methods. *Mol. Phys.* **1983**, *50*, 1055-1076.

32. Bussi, G.; Donadio, D. P., M. Canonical Sampling through Velocity Rescaling. *J. Chem. Phys.* **2007**, *126*, 14101-14107.

33. Essmann, U.; Perera, L.; Berkowitz, M. L.; Darden, T.; Lee, H.; Pedersen, L. G., A Smooth Particle Mesh Ewald Method. *J. Chem. Phys.* **1995**, *103*, 8577-8593

34. Hess, B.; Bekker, H.; Berendsen, H. J. C.; Fraaije, J. G. E. M., LINCS: A Linear Constraint Solver for Molecular Simulations. *J. Comput. Chem.* **1997**, *18*, 1463-1472.

35. Humphrey, W.; Dalke, A.; Schulten, K., VMD: Visual Molecular Dynamics. *J. Mol. Graph.* **1996**, *14*, 33-8, 27-8

36. Olubiyi, O. O., and Strodel, B., Structures of the Amyloid β-Peptides $A\beta_{1-40}$ and $A\beta_{1-42}$ as Influenced by pH and a D-peptide. *J.Phys. Chem. B*, **2012**, *116*, 3280−3291.

37. Kabsch, W.; Sander, C. Dictionary of Protein Secondary Structure: Pattern Recognition of Hydrogen-Bonded and Geometrical Features. *Biopolymers* **1983**, *22*, 2577-637.

38. Smith, D. M.; Straatsma, T. P.; Squier, T. C., Retention of Conformational Entropy Upon Calmodulin Binding to Target Peptides is Driven by Transient Salt-Bridges. *Biophys J* **2012**, *103*, 1576-1584.

39.Martin, K.; Kushick J. N., Method for Estimating the Configurational Entropy of Macromolecules. *Macromolecules* **1981**, *14*, 325-332.

40.Matteo, C.; Hoefinger S,; and Zerbetto, F., Probing the Structure of Lysozyme–Carbon Nanotube Hybrids with Molecular Dynamics. *Chemistry-A European Journal* **2012**, *18*, 4308-4313.

41. Jose, J. C.; Chatterjee, P.; Sengupta, N., Cross dimerization of amyloid-beta and alphasynuclein proteins in aqueous environment: a molecular dynamics simulations study. *PloS one* **2014,** *9* (9), e106883.

42. Basdevant, N.; Weinstein, H.; Ceruso, M., Thermodynamic basis for promiscuity and selectivity in protein-protein interactions: PDZ domains, a case study. *Journal of the American Chemical Society* **2006,** *128* (39), 12766-77.

43. Walton, E. B.; Vanvliet, K. J., Equilibration of Experimentally Determined Protein Structures for Molecular Dynamics Simulation. *Physical review. E, Statistical, nonlinear, and soft matter physics* **2006**, *74*, 061901-8.

44. Genheden, S.; Ryde, U., Will Molecular Dynamics Simulations of Proteins ever Reach Equilibrium? *Physical chemistry chemical physics PCCP* **2012**, *14*, 8662-8677.

45. Luo, J.; Warmlander, S. K.; Graslund, A.; Abrahams, J. P., Human lysozyme inhibits the in vitro aggregation of Abeta peptides, which in vivo are associated with Alzheimer's disease. *Chemical communications* **2013,** *49*, 6507-6509.

46. Guo, J.; Li, J.; Zhang, Y.; Jin, X.; Liu, H.; Yao, X., Exploring the influence of carbon nanoparticles on the formation of beta-sheet-rich oligomers of IAPP(2)(2)(-)(2)(8) peptide by molecular dynamics simulation. *PloS one* **2013,** *8*, e65579.

47. Moores, B.; Drolle, E.; Attwood, S. J.; Simons, J.; Leonenko, Z., Effect of Surfaces on Amyloid Fibril Formation. *PLoS One* **2011**, *6*, e25954

48. Williams, T. L.; Serpell, L. C., Membrane and surface interactions of Alzheimer's Abeta peptide--insights into the mechanism of cytotoxicity. *The FEBS Journal* **2011**, *278*, 3905-3917.

49. Huang, F.; Wang, J.; Qu, A.; Shen, L.; Liu, J.; Liu, J.; Zhang, Z.; An, Y.; Shi, L., Maintenance of Amyloid Beta Peptide Homeostasis by Artificial Chaperones Based on Mixed-Shell Polymeric Micelles. *Angewandte Chemie* **2014**, *34*, 8985-8990.

Graphical Abstract